Smart Handover for Hybrid LiFi and WiFi Networks

Xiping Wu, *Member, IEEE*, Dominic C. O'Brien, *Member, IEEE*, Xiong Deng, *Member, IEEE*, and Jean-Paul M. G. Linnartz, *Fellow, IEEE*

***Abstract*— This work investigates handover in hybrid light fidelity (LiFi) and wireless fidelity (WiFi) networks (HLWNets). In such a network, the handover process becomes challenging due to two main factors: i) the relatively short coverage range of a single access point (AP), and ii) the largely overlapping coverage areas of different networks. As a result, HLWNets are susceptible to frequent handovers. To reduce the handover rate, the concept of handover skipping (HS) was introduced, which enables handovers between non-adjacent APs. However, conventional HS methods rely on knowledge about the user's trajectory, which is not readily available at the AP. In this paper, a novel HS scheme is proposed on the basis of reference signal received power (RSRP) and its rate of change, with an adaptive network preference adopted. Since RSRP is commonly used in the existing handover schemes, the proposed method requires no additional signalling between the user and the AP. Simulation results show that the new method can effectively reduce unnecessary handovers, especially those between LiFi and WiFi. Compared to the standard and trajectory-based handover schemes, the proposed method improves network throughput by up to about 120% and 30%, respectively.**

***Index Terms*— Light fidelity (LiFi), wireless fidelity (WiFi), hybrid network, handover skipping, reference signal received power (RSRP).**

I. Introduction

LIGHT fidelity (LiFi) [2] is a wireless communication technology complementary to wireless fidelity (WiFi), and has the potential to address the problem of spectrum scarcity in radio frequency (RF). Using light waves as signal bearers, LiFi is able to exploit the vast visible optical spectrum of ∼300 THz. Also, LiFi offers secure communication as light does not penetrate opaque structures. Recent research shows that with a single light-emitting diode (LED), LiFi can provide a data rate above 10 Gbps [3]. Like millimetre wave communications, LiFi is susceptible to channel blockages caused by opaque objects such as human bodies. Therefore, a hybrid LiFi and WiFi network (HLWNet) becomes a promising solution to future indoor wireless communications [4].

In practice, a WiFi access point (AP) covers an area about 20 m in diameter, and for LiFi it is only 2-3 m [5]. In such an ultra-dense network, mobile users may experience frequent handovers if the signal strength strategy (SSS) is used. This technique assigns the user to the AP providing the highest reference signal received power (RSRP). To prevent successive handovers, the standard handover algorithm in the long-term evolution (LTE) [6] applies hysteresis, which postpones the handover decision to a certain extent. However, this approach is designed to eliminate the ping-pong effect, but has limited effectiveness in reducing handovers in ultra-dense networks.

To avoid frequent handovers, the concept of handover skipping was proposed for ultra-dense networks [7]–[9]. The authors in [7] developed a topology-aware skipping scheme, based on the chord length of the cell. This method has to predict the user's trajectory in order to obtain the length of the movement path within the coverage area of a certain AP. A similar method was proposed in [8], with the application scope extended to multi-AP association. In [9], a velocity-aware handover approach was reported for heterogeneous networks. However, the above methods all rely on the user's trajectory, which is not readily available at the AP.

Motivated by this, an RSRP-based handover skipping scheme was proposed for LiFi networks in [10]. The basic concept is to use the rate of change in RSRP to indicate whether the user is moving towards the central area of an AP. In this paper the work is extended to HLWNets, which have two types of handovers: vertical handover (VHO) and horizontal handover (HHO). VHOs occur between different wireless access technologies, whereas HHOs are within the same technology. A VHO normally requires a much longer processing time than a HHO due to different media access control (MAC) protocols [11]. Another point worth noting is that in a HLWNet, the coverage areas of LiFi and WiFi largely overlap each other. This fact affects the handover process in two aspects. On the one hand, slowly-moving or stationary users prefer LiFi (if available) to achieve high data rates. On the other hand, fast-moving users prefer WiFi to avoid frequent handovers. Therefore, we propose an adaptive handover scheme that can adjust the network preference for HLWNets.

Manuscript received January 28, 2020; revised July 20, 2020; accepted August 23, 2020. Date of publication September 4, 2020; date of current version December 10, 2020. This work was supported by the European Union's Horizon 2020 Research and Innovation Programme (ELIoT) under Grant 825651. This article was presented in part at the IEEE International Conference on Communications 2020. The associate editor coordinating the review of this article and approving it for publication was J. Liu. *(Corresponding author: Xiping Wu.)*

Xiping Wu and Dominic C. O'Brien are with the Department of Engineering Science, University of Oxford, Oxford OX1 3PJ, U.K. (e-mail: xiping.wu@eng.ox.ac.uk; dominic.obrien@eng.ox.ac.uk).

Xiong Deng is with the Department of Electrical Engineering, Eindhoven University of Technology, 5600 Eindhoven, The Netherlands (e-mail: x.deng@tue.nl).

Jean-Paul M. G. Linnartz is with the Department of Electrical Engineering, Eindhoven University of Technology, 5600 Eindhoven, The Netherlands, and also with Signify (Philips Lighting) Research, 5656 Eindhoven, The Netherlands (e-mail: j.p.linnartz@tue.nl).

Color versions of one or more of the figures in this article are available online at https://ieeexplore.ieee.org.

Digital Object Identifier 10.1109/TWC.2020.3020160

Relative to the conference version [1], the novel contribution of this paper is two-fold: i) the handover rate and the coverage probability of the proposed method are theoretically derived and analysed; and ii) in addition to the regular deployment, a random deployment of WiFi APs is considered to present a comprehensive performance evaluation of the proposed method. The remainder of this paper is organised as follows. Section II gives the system model including the models of network deployment, channel, user mobility and light-path blockages. Related work is introduced in Section III, and the novel method is proposed in Section IV. The handover rate and coverage probability of the proposed method are theoretically analysed in Section V. Simulation results are presented in Section VI. Finally, conclusions are drawn in Section VII.

II. System Model

An indoor HLWNet is considered as shown in Fig. 1. The room area is divided into square regions, with each region containing one WiFi AP and a number of LiFi APs. The WiFi APs can be deployed in two modes: regular and random. With the regular mode, the WiFi APs are placed at the region centres. With the random mode, each region has a randomly located WiFi AP. The LiFi APs are fitted on the ceiling and arranged in a lattice topology. The WiFi APs use carrier sense multiple access/collision avoidance (CSMA/CA), whereas the LiFi APs employ a frequency reuse factor of 4 [12]. The received signal-to-interference-plus-noise ratio (SINR) is denoted by γ_i, where i is the AP index. Due to limited space, interested readers are referred to [1] for detailed channel models. The capacity of WiFi can be bounded by Shannon capacity. As for LiFi, γ_i is an electrical SINR for non-negative signals, for which a tighter bound can be found [13]. Denoting the bandwidth by B_i, the link capacity can be expressed as:

$$r_i = \begin{cases} \frac{B_i}{2}\log_2\left(1+\frac{e}{2\pi}\gamma_i\right), & \text{for LiFi} \\ B_i\log_2\left(1+\gamma_i\right), & \text{for WiFi.} \end{cases} \quad (1)$$

A. User Mobility

Typical mobility models include the Manhattan mobility, reference point group mobility [14], and random waypoint (RWP) [15]. The RWP is commonly used, where users move along a zigzag line from one waypoint to another one, with the waypoints randomly distributed. With the original RWP model [16], users move within a large outdoor area and alter the speed when arriving at each waypoint. The distance between waypoints is relatively short in an indoor scenario. Hence, the speed is considered to be constant for a short period. The user's movement during such a period is called an excursion. When the current excursion ends, the user chooses a new speed, completely independent of all history, and continues moving. Let v denotes the average speed. The user's speed is assumed to be uniformly distributed between 0 and $2v$.

B. Light-Path Blockage

Light-path blockages affect the link performance of a LiFi user in two aspects: i) how often blockages occur; and ii) how long blockages last. The first factor triggers handovers, while the second impairs link quality. As a result, blockages can be characterised by two parameters: occurrence rate and occupation rate [17]. The occurrence rate is defined as the average number of blockages that occur in a time unit. In practice, blockages could occur in an unpredictable way. To quantify the impact of blockages, we assume them to follow the Poisson point process, which is widely used to model random events such as the arrival of packages. The occupation rate is defined as the proportion of time during blockages. The blockages regarding different APs are assumed independent.

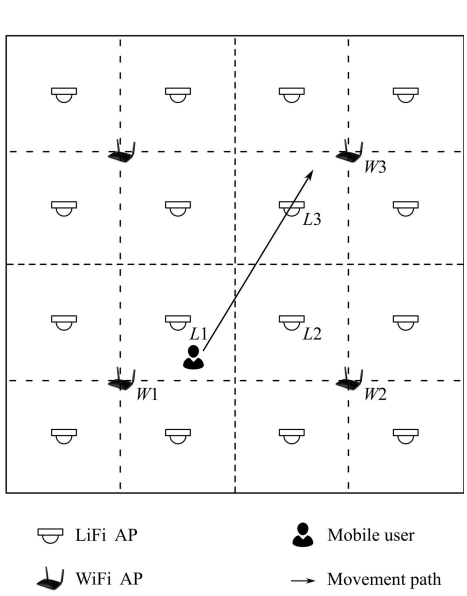

Fig. 1. Schematic of an indoor HLWNet.

III. Related Work

A. Standard Handover Scheme

To tackle the ping-pong effect, the handover scheme in LTE introduces two parameters: handover margin (HOM) and time to trigger (TTT). Fig. 2 presents the principle of this standard handover scheme, which is referred to as STD. The value of RSRP for the host AP is denoted by P_{i_H}, and for the target AP it is P_{i_T}. Let δ_{HOM} and t_{TTT} denote the values of HOM and TTT, respectively. The STD scheme starts counting time when the following condition is satisfied:

$$P_{i_T} > P_{i_H} + \delta_{\text{HOM}}. \quad (2)$$

The time counter continues as long as (2) is met, and otherwise is reset. When the counted time reaches t_{TTT}, a handover decision is then made to transfer the user from the host AP to the target AP. The STD scheme ensures a minimum connection time of t_{TTT}, which is usually restricted to hundreds of milliseconds [6]. For AP i, the traverse time is defined as the period from the time point where P_i becomes the largest to the time point where P_i is no longer the largest. For example, if the traverse time within $L2$ (in Fig. 1) is less than t_{TTT}, STD will transfer the user from $L1$ to $L3$, with $L2$ skipped. Otherwise the user will be transferred from $L1$ to $L2$, and then from $L2$ to $L3$. For STD, the ability of handover

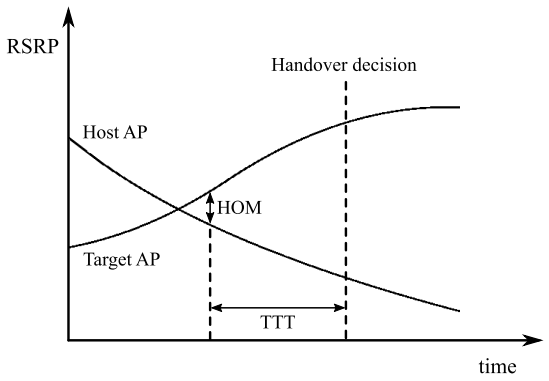

Fig. 2. The handover scheme in LTE.

skipping can be strengthened by increasing t_{TTT}. However, this will degrade the SINR performance.

B. Handover Skipping in a Homogeneous Network

To enable handover skipping without increasing t_{TTT}, it is required to predict the traverse time. Instead of reckoning the user's trajectory, the rate of change in RSRP can be used to indicate whether the user is moving towards the central area of an AP [10]. The user in Fig. 1 crosses the outskirts of $L2$ and moves towards the central area of $L3$. Therefore, $L3$ has a faster increase in RSRP than $L2$. The RSRP and its rate of change can be combined to determine whether an AP needs to be skipped. The objective function is written as [10, eq. (8)]:

$$\Gamma_i = P_i^{(t_0)} + \zeta \Delta P_i, \tag{3}$$

where t_0 is the starting point of the time counter; $P_i^{(t_0)}$ represents the RSRP of AP i at t_0; ζ is a weight coefficient, of which the optimal value has been proven to be 1 in [10]; ΔP_i is the rate of change in RSRP, and it is given by:

$$\Delta P_i = \frac{P_i^{(t_0+t_{\mathrm{TTT}})} - P_i^{(t_0)}}{t_{\mathrm{TTT}}}. \tag{4}$$

When the time counter reaches t_{TTT}, the AP providing the largest Γ_i will be chosen as the target AP. This approach requires RSRP information from APs in the detection range, which can be implemented in a way similar to STD.

IV. Proposed Handover Scheme

In a HLWNet, noise levels are different between LiFi and WiFi. Therefore, γ_i should be used instead of P_i. Fig. 3(a) presents the cellular topology of a HLWNet, where the border between two APs indicates that they have the same level of SINR. The borders between LiFi APs are straight lines, while the borders between LiFi and WiFi APs are slightly curvy. This is because with the same horizontal distance between the AP and the user, WiFi and LiFi provide different SINR levels. These slightly curvy borders can be approximated in straight lines, as shown in Fig. 3(b). The cell borders are fixed when (3) is used, resulting in frequent handovers for fast-moving users. For instance, though the user in Fig. 1 can skip $L2$, it will still be transferred from $W1$ to $L1$, then from $L1$ to $L3$, and finally from $L3$ to $W3$. However, it is better to transfer fast-moving users directly from $W1$ to $W2$. This can be realised by enlarging the WiFi region, as shown in Fig. 3(c). To achieve this, the objective function regarding WiFi is multiplied by a weight coefficient λ. Correspondingly, the objective function is expressed as:

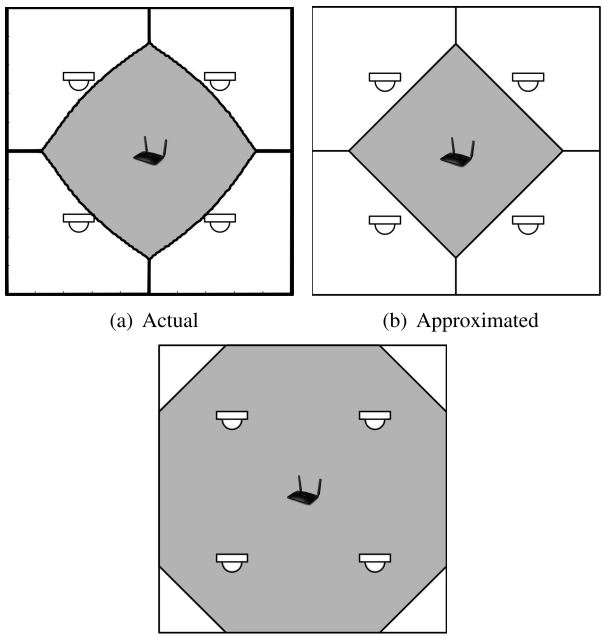

Fig. 3. The cellular topology of a HLWNet (The grey area is covered by WiFi, and the white area is covered by LiFi).

$$\Gamma_i = \begin{cases} \gamma_i^{(t_0)} + \Delta\gamma_i, & \text{for LiFi} \\ \lambda\left(\gamma_i^{(t_0)} + \Delta\gamma_i\right), & \text{for WiFi,} \end{cases} \tag{5}$$

where $\Delta\gamma_i$ is the SINR difference between the starting and ending points of the time counter:

$$\Delta\gamma_i = \frac{\gamma_i^{(t_0+t_{\mathrm{TTT}})} - \gamma_i^{(t_0)}}{t_{\mathrm{TTT}}}. \tag{6}$$

The coefficient λ is speed-dependent. When a user moves very slowly, λ should be 1 to let the user access the AP that offers the highest SINR. When the user moves fast, λ should be relatively large to reduce handovers. The impact and optimal selection of λ is studied in Section VI-A.

The proposed scheme counts time in a way similar to STD. When the time counter reaches t_{TTT}, the AP providing the largest Γ_i is chosen as the target AP, and a handover will be executed as soon as the target AP meets the condition in (2). If the user alters its moving direction or speed before the handover is made, the objective function in (5) will be recomputed to select a new target AP. Note that the target AP is not necessarily the one that triggers the time counter. For example, $L2$ (in Fig. 1) excites the time counter when the user crosses the border between $L1$ and $L2$, but the target AP could be $L3$. Though the illustrated path is a straight line, the proposed scheme applies to random movements since the path can be approximated to a straight line during a short

Algorithm 1 Proposed Handover Skipping Scheme

Input: $\gamma_{i_H}^{(t)}$, $\gamma_i^{(t)}$, $\forall i \in \mathcal{I}$
Output: i_T
$t_c \Leftarrow 0$
while $t_c < t_{\text{TTT}}$ **do**
  if $\gamma_i^{(t)} \leq \gamma_H^{(t)} + \delta_{\text{HOM}}, \forall i \in \mathcal{I}$ **then**
    $t_c \Leftarrow 0$
  else if $t_c = 0$ **then**
    $t_0 \Leftarrow t$
  else
    $t_c \Leftarrow t - t_0$
  end if
  $t \Leftarrow t + 1$
end while
if i is a LiFi AP **then**
  $\Gamma_i \Leftarrow \gamma_i^{(t_0)} + \left(\gamma_i^{(t_0+t_{\text{TTT}})} - \gamma_i^{(t_0)}\right)/t_{\text{TTT}}$
else if i is a WiFi AP **then**
  $\Gamma_i \Leftarrow \lambda\left[\gamma_i^{(t_0)} + \left(\gamma_i^{(t_0+t_{\text{TTT}})} - \gamma_i^{(t_0)}\right)/t_{\text{TTT}}\right]$
end if
$i_T \Leftarrow \max\{\Gamma_i\}$

period of t_{TTT}. Let γ_{i_H} denote the SINR value of the host AP. The output of the time counter is denoted by t_c. The target AP is denoted by i_T, while the set of all APs is denoted by $\mathcal{I}$. The pseudocode of the proposed scheme is given in Algorithm 1.

V. Theoretical Analysis of Handover Skipping Performance

In this section, the performance of the proposed scheme is theoretically analysed for an arbitrary line trajectory. A regular deployment of WiFi APs is considered without light-path blockages. The impact of a random deployment and blockages is studied numerically in Section VI. The handover rate depends on the cellular topology, which has two extreme cases, i.e. the WiFi region is null and the entire area. These cases are equivalent to a homogeneous LiFi or WiFi network, and the relevant analysis is referred to [10]. It is difficult to track the resulting change in performance when the situation varies between the above two cases. Alternatively, we analyse a special case where the WiFi region is half of the entire area.

A. Handover Rate

The handover rate of the proposed scheme can be measured by multiplying the handover rate of SSS by the probability of not skipping an AP. The handover rate of SSS is derived first. As shown in Fig. 3, the cellular topology is axisymmetric. Therefore, it can be assumed that the user enters one side of the square area at an arbitrary point (called an entry point) with an arbitrary angle. This angle is denoted by θ, and the distance between the entry point and a reference point is denoted by δ. Let d_{path} denote the length of the movement path within the region of an AP. The average value of d_{path} is denoted by $\bar{d}_{\text{path}}$, which is derived in Appendix VII-A. The handover rate of SSS, denoted by η, equals the speed v divided by $\bar{d}_{\text{path}}$:

$$\eta = \frac{3\pi v}{L}\left[\frac{7}{2}\log\left(\sqrt{2}+1\right) + \frac{1-\sqrt{2}}{2}\right]^{-1}. \tag{7}$$

Then we analyse the situation when the user does not skip an AP. This event is denoted by X and its probability is $\mathbb{P}(X)$. As shown in Fig. 11, there are two types of borders: i) between two LiFi APs and ii) between a LiFi AP and a WiFi AP. These two types are denoted by $B1$ and $B2$. The corresponding events are denoted by X_{B1} and X_{B2}, and their probabilities $\mathbb{P}(X_{B1})$ and $\mathbb{P}(X_{B2})$ are derived in Appendix VII-B. Then $\mathbb{P}(X)$ can be computed by:

$$\mathbb{P}(X) = \mathbb{P}(X_{B1})\mathbb{P}(B1) + \mathbb{P}(X_{B2})\mathbb{P}(B2), \tag{8}$$

where $\mathbb{P}(B1)$ and $\mathbb{P}(B2)$, the probabilities of $B1$ and $B2$, are proportional to the border length. We have $\mathbb{P}(B1) = \frac{1}{1+\sqrt{2}}$ and $\mathbb{P}(B2) = \frac{\sqrt{2}}{1+\sqrt{2}}$. The handover rate of the proposed method is the product of η and $\mathbb{P}(X)$, i.e. $\eta_{\text{HS}} = \eta\mathbb{P}(X)$.

B. Coverage Probability

The coverage probability measures the probability that the user's SINR is above a certain threshold, which is denoted by γ_T. Equivalently, the horizontal distance between the user and AP is below a certain threshold. For WiFi and LiFi, the distance thresholds are denoted by l_W and l_L. The WiFi channel commonly applies the log-distance path loss model [18, eq. (5)], and l_W can thus be readily obtained. The expression of l_L is given by [10, eq. (18)]. The coverage probability of SSS can be computed as follows:

$$\mathbb{P}(\gamma > \gamma_T) = \frac{\mathbb{A}(l < l_L) + \mathbb{A}(l < l_W)}{L^2}, \tag{9}$$

where $\mathbb{A}(l < l_L)$ and $\mathbb{A}(l < l_W)$ denote the areas where $l < l_L$ and $l < l_W$ are met. The corresponding expressions are written as (10) and (11), shown at the bottom of the next page.

The coverage probability of SSS is a function of L and is denoted by $\mathcal{P}(L)$. When the user does not skip an AP, the proposed method has the same coverage probability as SSS. Otherwise, the coverage probability is lower than SSS, since the value of $\bar{d}_{\text{path}}$ becomes larger. In this case, the coverage probability can be measured by replacing $\mathcal{P}(L)$ with $\mathcal{P}(\tilde{L})$, where $\tilde{L} = \bar{d}_{\text{HS}}L/\bar{d}_{\text{path}}$ and $\bar{d}_{\text{HS}}$ is the average length of the movement path within the coverage area of an AP when handover skipping occurs. The relation between $\bar{d}_{\text{HS}}$ and η_{HS} is written as follows:

$$\frac{v}{\eta_{\text{HS}}} = \mathbb{P}(X)\bar{d}_{\text{path}} + (1-\mathbb{P}(X))\bar{d}_{\text{HS}}. \tag{12}$$

Combining the above equation with $\eta_{\text{HS}} = \eta\mathbb{P}(X)$, it gives:

$$\bar{d}_{\text{HS}} = \frac{1+\mathbb{P}(X)}{\mathbb{P}(X)}\bar{d}_{\text{path}}. \tag{13}$$

The coverage probability of the proposed method can be obtained as follows:

$$\mathcal{P}_{\text{HS}}(L) = \mathbb{P}(X)\mathcal{P}(L) + (1-\mathbb{P}(X))\mathcal{P}\left(\frac{1+\mathbb{P}(X)}{\mathbb{P}(X)}L\right). \tag{14}$$

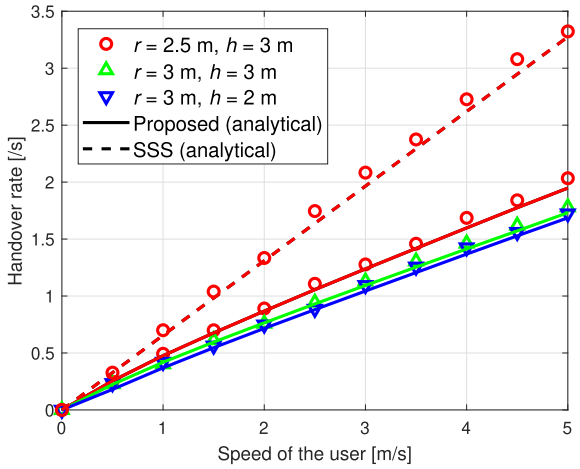

Fig. 4. Handover rate versus the user's speed.

C. Validation

Since the derivation of coverage probability is based on the handover rate, here we focus on verifying the theoretical analysis of the handover rate. The separation between the nearest LiFi APs is denoted by r, and the height between the user and LiFi APs is denoted by h. Fig. 4 shows the handover rate as a function of the user's speed. As can be seen, the analytical results match the simulations. The handover rate of the proposed method decreases when: i) r increases; and ii) h decreases. Also, the proposed method can greatly reduce the handover rate over SSS, especially for fast-moving users. This validates the ability of handover skipping that is provided by the proposed method.

VI. Simulation Results

Using Matlab, Monte Carlo simulations are conducted to evaluate the performance of the proposed method. We consider 4 WiFi APs and 16 LiFi APs. The separation between the nearest LiFi APs is set to be 2.5 m, and the vertical distance between the user and LiFi APs is 3 m. The bandwidth is assumed to be 10 MHz for each AP. The levels of transmission and noise power are referred to [18]. All LiFi APs are assumed to use the same level of transmission power, while power control for ultra-dense networks is feasible through methods such as [19]. The average overhead of HHO is about 200 ms in wireless local area networks (WLANs) [20], while the average overhead of VHO is set to be 500 ms [21]. Two baselines are considered: the STD and the trajectory-based handover skipping method in [7]. Here the STD scheme uses SINR instead of RSRP to suit the hybrid network. To provide a fair comparison, all methods use the same HOM and TTT, which are set to be 1 dB and 160 ms [6]. A single user is involved since the handover process is independent among users. The WiFi APs are regularly deployed unless otherwise stated.

A. Impact of the Weight Coefficient

In Fig. 5, the user throughput of the proposed method is presented as a function of the weight coefficient λ. For $v = 0.1$ m/s, the user throughput reaches a climax when $\lambda = 1$, as explained. The value of λ achieving the maximum throughput increases as v. Specifically, the optimal λ is 2 when $v = 1.5$ m/s. As for $v = 5$ m/s and 10 m/s, the user throughput gradually increases towards a saturation as λ approaches 10. Due to the complicated handover process, it is difficult to derive a closed-form expression of the optimal λ. Apart from that, in real life the network topology could be in any shape. However, we observe that the user throughput changes slowly near the vertex. (The only exception is when $v = 0.1$ m/s, where the best λ is readily determined to be 1.) Classifying the values of v, it is feasible to reach a sub-optimal λ through control systems such as fuzzy logic in practical applications.

With different deployments of the WiFi APs, the relation between the optimal λ and the user's speed is shown in Fig. 6. With an increase of v, the optimal λ increases very slightly until v reaches a certain point (1.5 m/s for the regular deployment and 2 m/s for the random deployment). Beyond this point, the optimal λ increases rapidly. This indicates that a large value of λ can benefit fast-moving users through enlarging the WiFi region. It is also found that when $v > 1$ m/s, the optimal λ of the random deployment is smaller than that of the regular deployment. This is because with the random deployment, a WiFi AP might be located near a LiFi AP and have a larger region than that of the regular deployment. As a result, the regular deployment needs to enlarge the WiFi region

$$\mathbb{A}(l < l_L) = \begin{cases} 2\pi l_L^2, & l_L \le \frac{L}{4} \\ L^2\sqrt{4\left(\frac{l_L}{L}\right)^2 - \frac{1}{4}} + l_L^2\left[2\pi - 8\arccos\left(\frac{L}{4l_L}\right)\right], & \frac{L}{4} < l_L \le \frac{L}{2} \\ \frac{L^2}{2}, & l_L > \frac{L}{2}. \end{cases} \tag{10}$$

$$\mathbb{A}(l < l_W) = \begin{cases} \pi l_W^2, & l_W \le \frac{L}{2\sqrt{2}} \\ L^2\sqrt{2\left(\frac{l_W}{L}\right)^2 - \frac{1}{4}} + l_W^2\left[\pi - 4\arccos\left(\frac{\sqrt{2}L}{4l_W}\right)\right], & \frac{L}{2\sqrt{2}} < l_W \le \frac{L}{2} \\ \frac{L^2}{2}, & l_W > \frac{L}{2}. \end{cases} \tag{11}$$

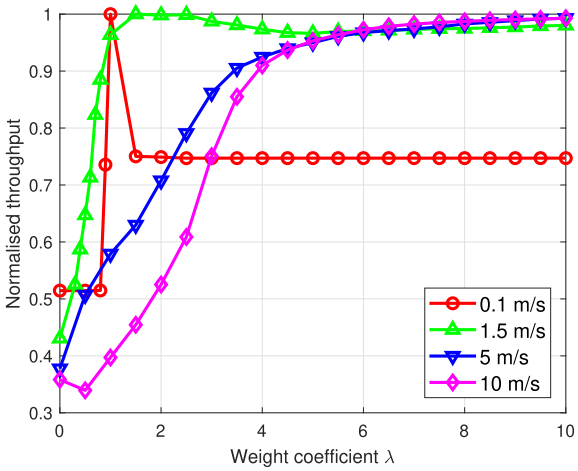

Fig. 5. User throughput versus the weight coefficient λ.

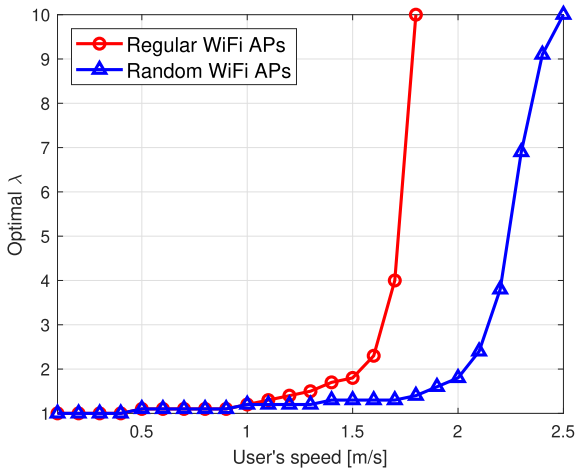

Fig. 6. Optimal weight coefficient λ versus the user's speed.

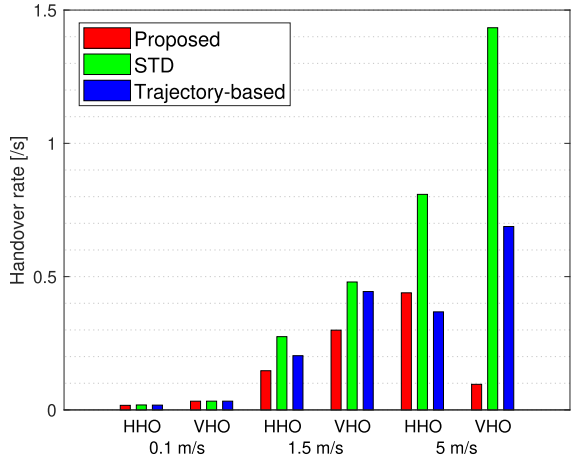

Fig. 7. Handover rates of HHO and VHO.

more significantly than the random deployment. The optimal values of λ are used in the following simulations.

B. Handover Rate

Fig. 7 shows the handover rates of HHO and VHO for different values of v. As can be seen, all methods achieve similar handover rates when $v = 0.1$ m/s. With a larger value

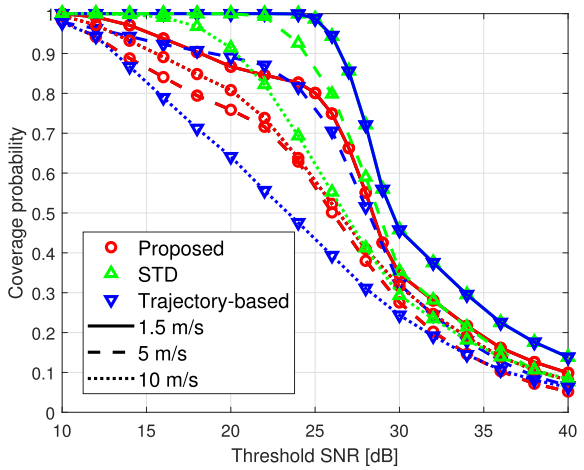

Fig. 8. Coverage probability for different speeds of the user.

of v, the proposed method provides the lowest handover rate, whereas STD has the highest. As v increases, in general, the handover rate increases for all methods. The only exception is that the VHO rate of the proposed method decreases when v increases from 1.5 m/s to 5 m/s. This is because the proposed method increases the WiFi region for fast-moving users, leading to fewer handovers between WiFi and LiFi. Consequently, the proposed method provides a much lower rate of VHO than STD and the trajectory-based method, with a decrease of 93% and 86%, respectively.

C. Coverage Probability

Fig. 8 presents the coverage probability for different values of v. Because of skipping some APs, the proposed method exhibits a lower coverage probability than STD, especially at the lower end of SINR values. Nonetheless, the SINR gap between the two methods is marginal at the 50-th percentile. When $v = 5$ m/s, for instance, the SINR values at the 50-th percentile are 26.0 dB and 28.6 dB for the proposed method and STD, resulting in an SINR gap of 2.6 dB. For $v = 1.5$ m/s, this SINR gap is only 1.2 dB.

D. Throughput

In Fig. 9, the user throughput is shown as a function of the user's speed. Three outcomes are observed. First, the proposed method and STD achieve almost the same throughput when v is below 1.5 m/s. This matches the fact that in the same range of v, the optimal λ of the proposed method is about 1. Second, as v further increases, the user throughput of the proposed scheme decreases much slower than that of other methods. At $v = 5$ m/s with the regular deployment, for example, the proposed method achieves a throughput of 71 Mbps, 122% and 29% higher than STD and the trajectory-based method, respectively. Third, the throughput gap between the proposed method and STD becomes smaller when the random deployment is applied instead of the regular deployment. Despite this, the proposed method can still improve the user throughput over STD by up to 72%.

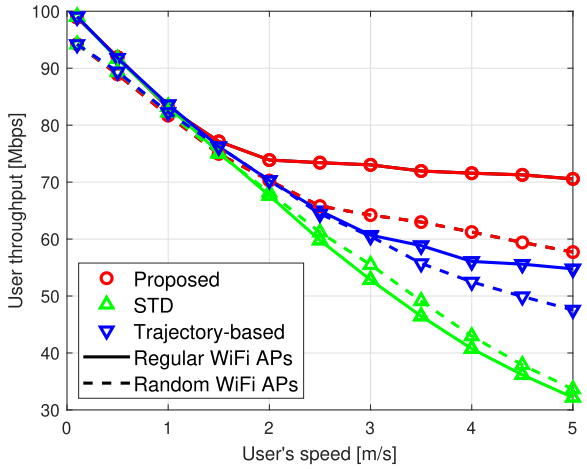

Fig. 9. User throughput versus the user's speed.

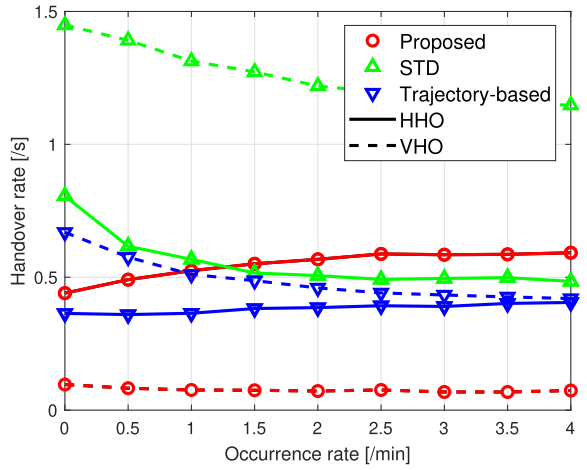

Fig. 10. Handover rate versus the occurrence rate of light-path blockages.

E. Impact of Light-Path Blockages

Finally, we investigate the effects of light-path blockages on the handover rate. Taking $v = 5$ m/s as an example, Fig. 10 shows the handover rate as a function of the occurrence rate of blockages, while the occupation rate is randomly chosen between 0 and 1 with a uniform distribution. Regarding STD, the rates of HHO and VHO both noticeably decrease as the occurrence rate increases. This is because during light-path blockages, the user has to be served by WiFi. As a result, the HHO rate related to LiFi reduces, as well as the VHO rate. In contrast, the proposed method has an increased HHO rate with a barely changed VHO rate, but the overall handover rate is still much lower than that of STD. In the extreme case of a continuous blockage, the hybrid network would reduce to a homogeneous WiFi network, and all handover methods would have no VHOs.

The performance analysis in this section is undertaken with perfect SINR information. In practice, SINR measurement errors and delays are inevitable. This would result in early or late handover implementations but have little impact on the handover rate, attributed to the use of hysteresis. The user throughput would be degraded to some extent due to two main factors: unpunctual handovers and channel estimation errors.

VII. Conclusion

In this paper, a novel handover scheme was proposed for HLWNets. Unlike the trajectory-based handover skipping method, the proposed scheme combines SINR and its rate of change to determine whether an AP should be skipped. Also, the proposed method employs a dynamic network preference, which is adaptive to the user's velocity. Specifically, fast-moving users are likely to be served by WiFi in order to avoid frequent handovers. In contrast, slowly-moving users prefer the AP that provides the highest SINR. Results show that compared to the standard handover scheme, the new method can reduce the handover rate by 40% at a walking speed and over 70% at a running speed. In terms of user throughput, the proposed method can provide an increase of up to 120% against the standard scheme and 30% against the trajectory-based method.

Appendix

A. Derivation of $\bar{d}_{path}$

There are four types of movement paths, as demonstrated in Fig. 11. Let L denote the side length of the entire area. The length of the movement path within the entire area is denoted by d_{tot}, which can be expressed as follows:

$$d_{\text{tot}}(\delta) = \begin{cases} \dfrac{\delta}{\cos(\theta)}, & 0 \le \theta < \theta_1 \\ \dfrac{L}{\sin(\theta)}, & \theta_1 \le \theta < \dfrac{\pi}{2} \\ \dfrac{L}{\sin(\pi-\theta)}, & \dfrac{\pi}{2} \le \theta < \theta_2 \\ \dfrac{L-\delta}{\cos(\pi-\theta)}, & \theta_2 \le \theta \le \pi, \end{cases} \tag{15}$$

where:

$$\begin{cases} \theta_1 = \arctan\left(\dfrac{L}{\delta}\right) \\ \theta_2 = \pi - \arctan\left(\dfrac{L}{L-\delta}\right). \end{cases} \tag{16}$$

The second and third types can be merged, since $\sin(\theta) = \sin(\pi - \theta)$. Let N_{AP} denote the number of APs that the user goes through. For each possible path, the value of d_{path} equals d_{tot} divided by N_{AP}, which can be computed as follows:

$$N_{\text{AP}} = \begin{cases} 1, & 0 \le \theta < \theta_3 \\ 3, & \theta_3 \le \theta \le \pi, \end{cases} \tag{17}$$

where:

$$\theta_3 = \arctan\left(\frac{L}{2\delta}\right). \tag{18}$$

Thus, d_{path} is given by:

$$d_{\text{path}}(\delta) = \begin{cases} \dfrac{\delta}{\cos(\theta)}, & 0 \le \theta < \theta_3 \\ \dfrac{\delta}{3\cos(\theta)}, & \theta_3 \le \theta < \theta_1 \\ \dfrac{L}{3\sin(\theta)}, & \theta_1 \le \theta < \theta_2 \\ \dfrac{L-\delta}{3\cos(\pi-\theta)}, & \theta_2 \le \theta \le \pi. \end{cases} \tag{19}$$

$$\bar{d}_{\text{path}}(\delta) = \frac{1}{\pi}\left(\int_{\theta=0}^{\theta_3} \frac{\delta}{\cos(\theta)}d\theta + \int_{\theta=\theta_3}^{\theta_1} \frac{\delta}{3\cos(\theta)}d\theta + \int_{\theta=\theta_1}^{\theta_2} \frac{L}{3\sin(\theta)}d\theta + \int_{\theta=\theta_2}^{\pi} \frac{\delta - L}{3\cos(\theta)}d\theta\right). \tag{20}$$

$$\bar{d}_{\text{path}}(\delta) = \frac{1}{3\pi}\left[2\delta\log\left(\frac{L+2\delta_3}{2\delta}\right) + \delta\log\left(\frac{L+\delta_1}{\delta}\right) + L\log\left(\frac{\delta+\delta_1}{\delta_2 - L + \delta}\right) + (L-\delta)\log\left(\frac{L+\delta_2}{L-\delta}\right)\right]. \tag{21}$$

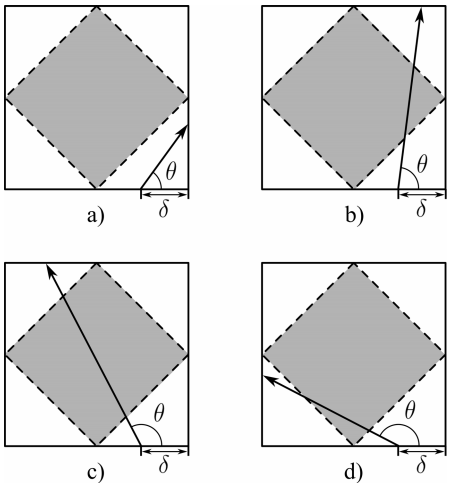

Fig. 11. User's movement paths (grey areas: WiFi regions; solid lines: borders between LiFi APs; dashed lines: borders between a LiFi AP and a WiFi AP).

The average value of $d_{\text{path}}(\delta)$ is calculated by (20) shown at the top of this page. The integrals on the right side of (20) can be solved by calculating the antiderivatives. As a result, (20) can be rewritten as (21) shown at the top of this page, where:

$$\begin{cases} \delta_1 = \sqrt{\delta^2 + L^2} \\ \delta_2 = \sqrt{(L-\delta)^2 + L^2} \\ \delta_3 = \sqrt{\delta^2 + (L/2)^2}. \end{cases} \tag{22}$$

Since δ varies between 0 and $\frac{L}{2}$, $\bar{d}_{\text{path}}$ can be calculated as follows:

$$\bar{d}_{\text{path}} = \frac{2}{L}\int_{\delta=0}^{\frac{L}{2}} \bar{d}_{\text{path}}(\delta)d\delta. \tag{23}$$

Substituting (21) into (23), $\bar{d}_{\text{path}}$ is obtained as follows:

$$\bar{d}_{\text{path}} = \frac{L}{3\pi}\left[\frac{7}{2}\log\left(\sqrt{2}+1\right) + \frac{1-\sqrt{2}}{2}\right]. \tag{24}$$

B. Derivation of $\mathbb{P}(X_{B1})$ and $\mathbb{P}(X_{B2})$

Fig. 12 shows the situation when the user crosses border $B1$ and enters region T. As shown, there are six APs that can possibly replace T as the target AP. The corresponding regions are denoted by A_k, where $k = 1, 2, \ldots, 6$. Other APs are less likely to become the target AP since they provide a much smaller SINR. The event X_{B1}, i.e. the user does not skip

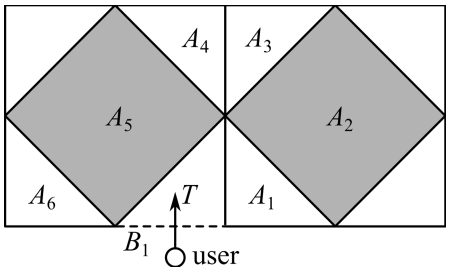

Fig. 12. The user crosses border $B1$ (dashed line).

T, occurs when Γ_T is the largest among all APs. Therefore, $\mathbb{P}(X_{B1})$ can be expressed as:

$$\mathbb{P}(X_{B1}) = \mathbb{P}(\Gamma_T \geq \Gamma_{A_k}, \forall k). \tag{25}$$

According to [10, eq. (40)], we have:

$$\mathbb{P}(\Gamma_T \geq \Gamma_{A_k} \mid \theta, \delta) = \begin{cases} 0, & \Theta_{A_k} \leq \theta < \hat{\Theta}_{A_k} \\ 1, & \text{otherwise}, \end{cases} \tag{26}$$

where Θ_{A_k} and $\hat{\Theta}_{A_k}$ are the smallest and largest angles that enable A_k to replace T as the target AP. These angles depend on δ, and can be determined by the used channel model. Unfortunately, it is difficult to derive closed-form expressions of Θ_{A_k} and $\hat{\Theta}_{A_k}$, due to their high orders in the channel model. Alternatively, they can be obtained numerically. Since θ is uniformly distributed between 0 and π, we have:

$$\mathbb{P}(X_{B1} \mid \delta) = 1 - \frac{1}{\pi}\sum_k \left(\hat{\Theta}_{A_k}(\delta) - \Theta_{A_k}(\delta)\right). \tag{27}$$

The probability $\mathbb{P}(X_{B1})$ can be computed as follows:

$$\mathbb{P}(X_{B1}) = \int_\delta \mathbb{P}(X_{B1} \mid \delta)\mathbb{P}(\delta)d\delta. \tag{28}$$

Since δ is uniformly distributed between 0 and $\frac{L}{2}$, we have $\mathbb{P}(\delta) = \frac{2}{L}$. Substituting (27) into (28), $\mathbb{P}(X_{B1})$ is given by:

$$\mathbb{P}(X_{B1}) = \frac{2}{L}\int_{\delta=0}^{\frac{L}{2}} 1 - \frac{1}{\pi}\sum_k \left(\hat{\Theta}_{A_k}(\delta) - \Theta_{A_k}(\delta)\right)d\delta. \tag{29}$$

The probability $\mathbb{P}(X_{B2})$ can be derived in a similar way. The details are omitted here due to limited space.

REFERENCES

[1] X. Wu and D. O'Brien, "A novel handover scheme for hybrid LiFi and WiFi networks," in *Proc. IEEE Int. Conf. Commun. (ICC)*, Jun. 2020, pp. 1–5.

[2] H. Haas, L. Yin, Y. Wang, and C. Chen, "What is LiFi?" *J. Lightw. Technol.*, vol. 34, no. 6, pp. 1533–1544, Mar. 15, 2016.

[3] M. S. Islim *et al.*, "Towards 10 Gb/s orthogonal frequency division multiplexing-based visible light communication using a GaN violet micro-LED," *Photon. Res.*, vol. 5, no. 2, p. A35, Apr. 2017.
[4] X. Wu, M. D. Soltani, L. Zhou, M. Safari, and H. Haas, "Hybrid LiFi and WiFi networks: A survey," 2020, *arXiv:2001.04840*. [Online]. Available: http://arxiv.org/abs/2001.04840
[5] H. Haas, "Visible light communication," in *Proc. Opt. Fiber Commun. Conf. Exhib. (OFC)*, Los Angeles, CA, USA, 2015, pp. 1–72.
[6] *LTE; Evolved Universal Terrestrial Radio Access (E-UTRA); Radio Resource Control (RCC); Protocol Specification (Release 13)*, Standard 3GPP TS 36.331 v13.0.0., Tech. Rep., Valbonne, France, Jan. 2016.
[7] R. Arshad, H. Elsawy, S. Sorour, T. Y. Al-Naffouri, and M.-S. Alouini, "Handover management in 5G and beyond: A topology aware skipping approach," *IEEE Access*, vol. 4, pp. 9073–9081, 2016.
[8] E. Demarchou, C. Psomas, and I. Krikidis, "Mobility management in ultra-dense networks: Handover skipping techniques," *IEEE Access*, vol. 6, pp. 11921–11930, 2018.
[9] R. Arshad, H. ElSawy, S. Sorour, T. Y. Al-Naffouri, and M.-S. Alouini, "Velocity-aware handover management in two-tier cellular networks," *IEEE Trans. Wireless Commun.*, vol. 16, no. 3, pp. 1851–1867, Mar. 2017.
[10] X. Wu and H. Haas, "Handover skipping for LiFi," *IEEE Access*, vol. 7, pp. 38369–38378, 2019.
[11] *Requirements for Evolved UTRA (E-UTRA) and Evolved UTRAN (E-UTRAN) (Release 9)*, Standard TR 25.913, 3GPP, Tech. Rep., Valbonne, France, Dec. 2009.
[12] X. Wu and D. C. O'Brien, "Parallel transmission LiFi," *IEEE Trans. Wireless Commun.*, early access, Jun. 19, 2020, doi: 10.1109/TWC.2020.3001983.
[13] J.-B. Wang, Q.-S. Hu, J. Wang, M. Chen, and J.-Y. Wang, "Tight bounds on channel capacity for dimmable visible light communications," *J. Lightw. Technol.*, vol. 31, no. 23, pp. 3771–3779, Dec. 2013.
[14] X. Hong, M. Gerla, G. Pei, and C. C. Chiang, "A group mobility model for ad hoc wireless networks," in *Proc. 2nd ACM Int. Workshop Modeling, Anal. Simulation Wireless Mobile Syst. (MSWiM)*, Seattle, WA, USA, 1999, pp. 53–60.
[15] D. Johnson and D. Maltz, "Dynamic source routing in ad hoc wireless networks," in *Mobile Computing*. New York, NY, USA: Springer, 1996, pp. 153–181.
[16] W. Navidi and T. Camp, "Stationary distributions for the random waypoint mobility model," *IEEE Trans. Mobile Comput.*, vol. 3, no. 1, pp. 99–108, Jan. 2004.
[17] X. Wu and H. Haas, "Load balancing for hybrid LiFi and WiFi networks: To tackle user mobility and light-path blockage," *IEEE Trans. Commun.*, vol. 68, no. 3, pp. 1675–1683, Mar. 2020.
[18] X. Wu and H. Haas, "Mobility-aware load balancing for hybrid LiFi and WiFi networks," *IEEE/OSA J. Opt. Commun. Netw.*, vol. 11, no. 12, pp. 588–597, Dec. 2019.
[19] L. Xiao *et al.*, "Reinforcement learning-based downlink interference control for ultra-dense small cells," *IEEE Trans. Wireless Commun.*, vol. 19, no. 1, pp. 423–434, Jan. 2020.
[20] J. Xiao and F. Liu, "A pre-scanning fast handoff scheme for VoIP in WLANs," *Int. J. Future Gener. Commun. Netw.*, vol. 8, no. 2, pp. 343–354, Apr. 2015.
[21] H. Kwon, K.-Y. Cheon, and A. Park, "Analysis of WLAN to UMTS handover," in *Proc. IEEE 66th Veh. Technol. Conf.*, Sep. 2007, pp. 184–188.

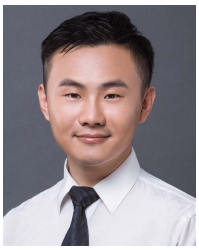

Xiping Wu (Member, IEEE) received the Ph.D. degree from the University of Edinburgh, U.K., in 2015. From 2011 to 2014, he was a Marie-Curie Early-Stage Researcher, funded by the European Union's Seventh Framework Program (FP7). From 2015 to 2018, he held a Post-Doctoral Fellowship with The University of Edinburgh, funded by the British EPSRC (Engineering and Physical Sciences Research Council). He is currently a Research Fellow with the University of Oxford. His main research interests are in the areas of optical wireless communications, hybrid OWC and RF networks, and the Internet of Things.

Dominic C. O'Brien (Member, IEEE) is currently a Professor of engineering science at Oxford and leads the Optical Communications Group. He is also the Director of the U.K. Quantum Technology Hub in Quantum Computing and Simulation. He has a range of experience in optoelectronics research in industry (BT labs) and academia. He has authored or coauthored approximately 200 publications in this area. The group has a wide range of experience in free-space optical communications and optical wireless, demonstrating integrated optical wireless transceivers, full room-scale systems at 300 Mbit/s, and integrated visible-light communications systems.

Xiong Deng (Member, IEEE) received the M.Eng. degree in communication and information engineering from the University of Electronic Science and Technology of China, in 2013, and the Ph.D. degree in optical wireless communications from the Eindhoven University of Technology in 2018. In 2013, he was a Researcher with the Terahertz Science and Technology Research Center, China Academy of Engineering Physics, where he was involved in the integrated terahertz communication and imaging system. He was a Guest Researcher with Signify (Philips Lighting) Research, where he was involved in light fidelity. He is currently a Post-Doctoral Researcher with the Eindhoven University of Technology. His research interests include system modeling, digital signal processing, and circuits for intelligent lighting, millimeter wave, radio over fiber, and optical wireless communications. He serves as a Reviewer for multiple IEEE/OSA journals, including the IEEE TRANSACTIONS ON INDUSTRIAL ELECTRONICS, the IEEE JOURNAL OF EMERGING AND SELECTED TOPICS IN INDUSTRIAL ELECTRONICS, the IEEE TRANSACTIONS ON COMPUTERS, the IEEE TRANSACTIONS ON VEHICULAR TECHNOLOGY, *Journal of Lightwave Technology*, the IEEE TRANSACTIONS ON COGNITIVE COMMUNICATIONS AND NETWORKING, the IEEE COMMUNICATIONS LETTERS, and the IEEE PHOTONICS JOURNAL.

Jean-Paul M. G. Linnartz (Fellow, IEEE) was an Assistant Professor with the University of California at Berkeley. In 1994, he was Associate Professor with TU Delft from 1992 to 1995. He is currently a Research Fellow with Signify (Philips Lighting) and a part-time Professor with Eindhoven University of Technology (TU Eindhoven). As a Senior Director with Philips Research, Eindhoven, he headed the Security and Connectivity and IC Design Research Groups. His inventions led to more than 75 granted patents and have been a basis for three successful ventures. His work has been cited over 11 000 times (Google Scholar). He is a fellow of the IEEE for leadership in security with noisy data.